

Copyright 2006 Society of Photo-Optical Instrumentation Engineers.

This paper will be published in Sensors, and Command, Control, Communications, and Intelligence (C3I) Technologies for Homeland Security and Homeland Defense V. Edited by Carapezza, Edward M..

Proceedings of the SPIE, Volume 6201 and is made available as an electronic reprint (preprint) with permission of SPIE. One print or electronic copy may be made for personal use only. Systematic or multiple reproduction, distribution to multiple locations via electronic or other means, duplication of any material in this paper for a fee or for commercial purposes, or modification of the content of the paper are prohibited.

Detection and localization of persons behind obstacles using M-sequence through-the-wall radar

Rudolf Zetik^{*a}, Stephen Crabbe^b, Jozef Krajnak^c, Peter Peyerl^d, Jürgen Sachs^a, Reiner Thomä^a

^aIlmenau University of Technology, Dept. EEIT, P.O.B. 100565, 98684 Ilmenau, Germany;

^bStephen Crabbe Consulting, Allerheiligenstr. 17, 99084 Erfurt, Germany;

^cTechnical University of Kosice, Letna 9, 042 00 Kosice, Slovakia;

^dMEODAT GmbH, Werner-von-Siemens-Str. 3, 98693 Ilmenau, Germany

ABSTRACT

We describe the architecture and design of a through-the-wall radar. The radar is applied for the detection and localization of people hidden behind obstacles. It implements a new adaptive processing technique for people detection, which is introduced in this article. This processing technique is based on exponential averaging with adopted weighting coefficients. Through-the-wall detection and localization of a moving person is demonstrated by a measurement example. The localization relies on the time-of-flight approach.

Keywords: Detection of people, localization, through-the-wall radar, UWB systems

1. INTRODUCTION

There are a number of situations where the entering of a room or a building is considered hazardous and it is desired to inspect the interior from outside through walls. An example includes the tracking of people in dangerous environments. Search and rescue workers would benefit greatly from through-the-wall imaging in time critical events such as fire rescue or collapsed buildings. Law enforcement also often faces the task of determining the exact locations of people behind walls in hostage scenarios. Specialized devices using electromagnetic waves can provide significant help in these applications [1], [2], [3], [4], [5]. Here, the electromagnetic waves propagate through walls and other non-conducting obstacles. Changes in the propagation medium induce reflections of the electromagnetic waves and can indicate objects of interest (human beings), which can then be detected by radar, and thus the operator.

The goal of this article is to describe architecture and design of an ultra-wideband (UWB) through-the-wall radar and its application for the detection and localization of people. This radar uses binary sequences (M-sequences) to stimulate the scenario. It operates in the frequency band from approximately 700MHz (constrained by antenna used) to 4.5GHz. It detects and localises people by means of electromagnetic waves reflected from their bodies also if they are hidden behind obstacles such as walls, or debris. Electromagnetic waves reflected from people are however weak in comparison to the cross-talk between transmit and receive antenna, or to waves scattered from walls, furniture, etc. Therefore, it is essential to separate these weak reflected waves by appropriate algorithms. This is usually achieved by “background subtraction” algorithms. These algorithms are known from the area of the automated visual surveillance [6], [7], or from radar signal processing [8] for the detection of small objects such as e.g. mines [9]. This article introduces an adaptive background subtraction technique. This technique is based on exponential averaging and was developed with the focus on the people detection. Its performance and subsequent people localization ability will be demonstrated by measurement examples using a M-sequence radar.

2. DETECTION OF PEOPLE

The most challenging part in the location and positioning of persons is their detection. The goal is to differentiate electromagnetic waves scattered from a person and waves arising from antenna cross-talk or scattered from other objects. In order to illustrate how challenging this task is, let us assume following scenario.

* rudolf.zetik@tu-ilmenau.de; phone +49 (0)3677 691160; fax +49 (0)3677 691113

We have one transmit antenna Tx and one receive antenna Rx. These antennas are in a lossless medium (air) and are static during the measurement. We will consider only one person, which should be detected and no other object (see Fig. 1).

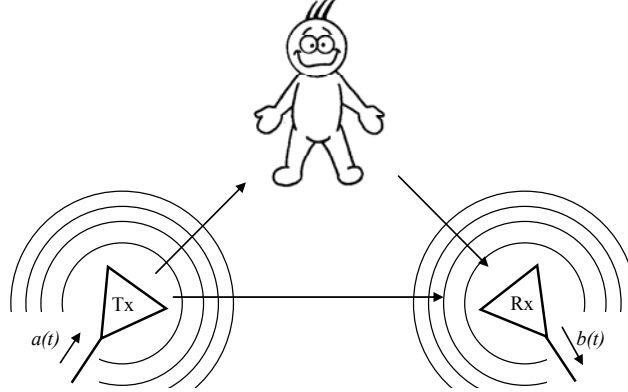


Fig. 1 Propagation of electromagnetic waves

The person is situated R_T meters from the transmit antenna Tx and R_R meters from the receive antenna Rx. If the antenna Tx transmits electromagnetic waves then the normalized incident electromagnetic field $c_i(t, R_T)$ at distance R_T from the antenna Tx, i.e. at the position of the person is

$$(1) \quad c_i(t, R_T) = \frac{1}{2\pi R_T} a\left(t - \frac{R_T}{c}\right) \otimes g_T(t) \quad ,$$

where \otimes stands for the convolution, $a(t)$ is the normalized electromagnetic wave stimulating the antenna Tx, c is the speed of electromagnetic waves in air, $g_T(t)$ is the transmit antenna response function. Generally, it is angle dependent. Thus, the waveform of transmitted electromagnetic waves varies with azimuth and elevation. Here, for the sake of simplicity, we will not consider azimuth and elevation as parameters of this function. As the transmitted electromagnetic waves reach the person, the body itself becomes the source of reflected electromagnetic waves and the normalized scattered electromagnetic field $c_s(t, R_R)$ at distance R_R from the person, i.e. at the position of the receive antenna Rx is

$$(2) \quad c_s(t, R_R) = \frac{1}{2\pi R_R} c_i(t, R_T) \otimes o(t, \varphi, \theta) \otimes \delta\left(t - \frac{R_R}{c}\right) \quad ,$$

where $\delta(t)$ is the Dirac impulse function, $o(t)$ is the impulse response function of the object (person), which describes the ability of the person to reflect electromagnetic waves as well as the antenna response function, the object response function is angle dependent. The waveform of scattered electromagnetic waves varies with azimuth and elevation of incident waves as well as with azimuth and elevation of scattered waves. For the sake of simplicity, we will not consider angle variables as parameters of this function.

The electromagnetic waves received by the antenna Rx that are caused only by the reflection at the person are described as follows

$$(3) \quad b_s(t) = c_s(t, R_R) \otimes g_R(t) \quad .$$

Here, $g_R(t)$ is the receive antenna response function, which is angle dependent. The receive antenna response function is not identical with the transmit antenna response function. However, due to the principle of reciprocity, there is relation between these two response functions. More details can be found in [10].

The total electromagnetic wave obtained from the receive antenna Rx is a combination of the antenna cross-talk – a direct wave propagating from the transmit antenna Tx directly to the receive antenna Rx and the electromagnetic waves reflected back from the person. Thus, the total electromagnetic wave measured by the receive antenna is

$$(4) \quad b_T(t) = \frac{1}{2\pi R} a\left(t - \frac{R}{c}\right) \otimes g_T(t) \otimes g_R(t, \varphi, \theta) + \frac{1}{4\pi^2 R_T R_R} a\left(t - \frac{R_R + R_T}{c}\right) \otimes g_T(t) \otimes o(t) \otimes g_R(t) \quad .$$

Here, only the second term related to the reflected electromagnetic waves is used for the detection of the targeted person. The antennas Tx and Rx are usually co-located in an array. Thus, the power of the antenna cross-talk is huge in comparison to the power of the electromagnetic waves reflected back from the person standing tens of meters away from the antenna array. Therefore, through-the-wall radar must be able to differentiate between the waves reflected back from the targeted person and the antenna cross-talk together with the backscattered waves from other objects.

If we assume that the radar's dynamic range is high enough to cover the power differences between the strong cross-talk signal and the weak signals coming from the targeted persons, then the detection still depends on various conditions such as:

- the number of persons to be detected, localized and tracked,
- their activity,
- environmental conditions and others.

The person's activity is characterised by their movement (walking, or sitting). This significantly influences their detection. A moving person is easily to detect in comparison to the sitting or laying person. In the latter case, the person can be detected only according its respiratory or heartbeat activity. Respiratory and heartbeat activity is, however, a challenging task especially in case where persons are situated behind obstacles.

Environmental conditions also determine the degree of complexity of the person's detection. It is reflected by its temporal changes in the scenario. If all objects in the person's surroundings are static then the detection of a moving person is relatively easy. In this case, the targeted person can be differentiated from other objects in its surroundings according its movement. In the case where the scenario is time varying with various moving objects, person detection is a challenging task, since the detection of moving objects must be followed by the target recognition.

Thus, the easiest case for person detection is a static scenario and only one moving person. Within this article we will assume this scenario. Here, the detection can be performed by means of "background subtraction" algorithms. These algorithms subtract time invariant "background" of the static scenario from measured data. The "background" refers to a signal, which is contributed to in all measured impulse responses. It contains especially the antenna cross-talk and waves reflected from static objects. The idea behind the background subtraction algorithms is illustrated by the following example. Here, we assume one person moving along some trajectory and only one static object (see Fig. 2). Further, let us assume an UWB radar sends from the transmit antenna short impulses in a certain measurement rate. Transmitted electromagnetic waves propagate, firstly, directly to the receive antenna (blue solid line) and they are also back scattered from the static object (black semisolid lines) and from the person (red dashed lines), which appears to the radar at a certain time instant as a static object. Red circles situated along the person's trajectory represent subsequent positions of the moving person that are related to time instants when the radar transmits new impulses. Impulse responses recorded by the UWB radar for this scenario are shown in Fig. 3. Impulse responses are aligned to each other creating a 2 dimensional picture, where the vertical axis is related to the time delay of the impulse response and the horizontal axis is related to the measurement time. Thus, one vertical line from this 2 dimensional figure represents one impulse response. Direct waves propagating from the transmit antenna Tx to the receive antenna Rx are illustrated by blue unipolar monopulse, scattering from the static object is shown as a black bipulse and the waves scattered from the moving person are depicted by the red bipolar monopulse.

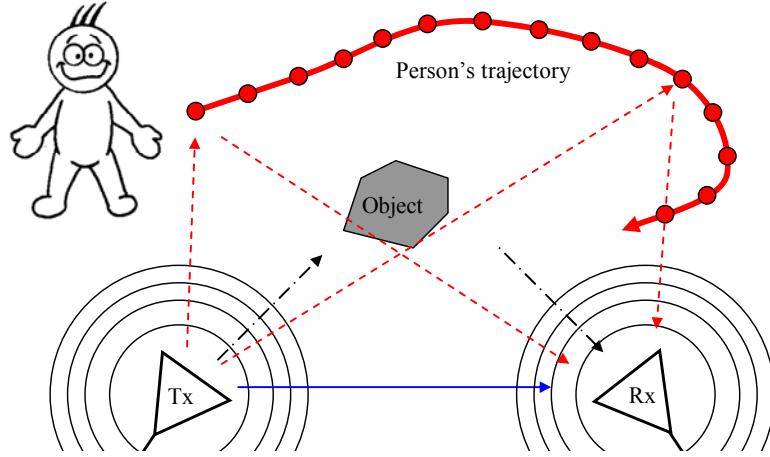


Fig. 2 Detection of a moving person in the case of a static scenario

From the figure, it is obvious that the direct wave and the scattering from the static object create horizontal lines parallel to the time axis. In order to remove scattering from static objects we have to estimate this time-invariant background and subtract it from measured data. The ideal result of the background subtraction algorithm is depicted in Fig. 4. In real situations, there is always some estimation error while estimating the background. Thus, signals coming from the antenna cross-talk and static signals are never completely removed and produce some distortion in the resulting image. The level of this distortion depends on the particular approach used for the background estimation.

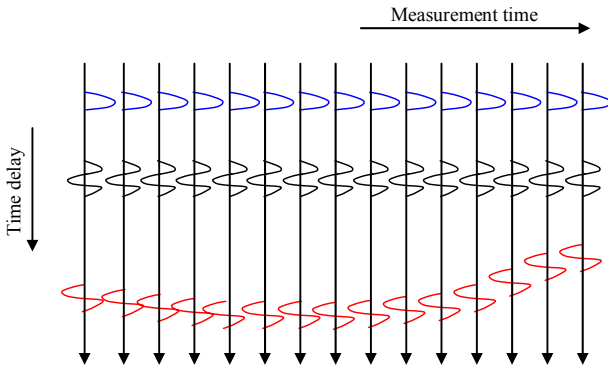


Fig. 3 Measured data

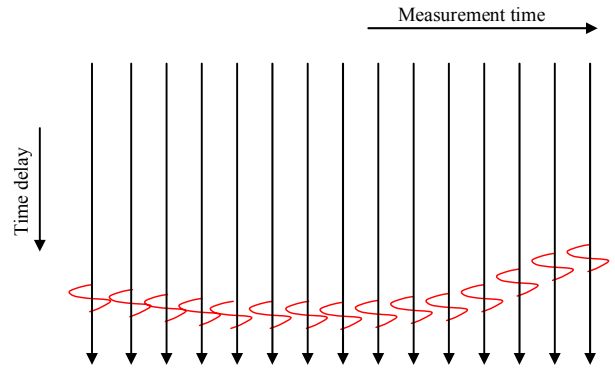


Fig. 4 Data after background subtraction

There are different approaches as to how to estimate the background. The easiest way is to compute an averaged impulse response from all measured impulse responses. However, this approach is only suitable for off-line processing when the measurement is completed and there is an access to all measured impulse responses. Another approach applies exponential averaging. Here, the new background estimate y_k is computed from the previous background y_{k-1} estimation that is updated with the new measured impulse response x_k according to the following equation:

$$(5) \quad y_k = \alpha y_{k-1} + (1-\alpha)x_k = y_{k-1} + (1-\alpha)(x_k - y_{k-1}) = y_{k-1} + (1-\alpha)z_k$$

where α is the constant scalar weighing factor, y_k and x_k are one dimensional vectors with the size $[N \times 1]$ and contain sampled background estimate and measured impulse response, respectively. Index k refers to the actual time instant. Thus, new background estimate takes a fraction of the previous estimate and a fraction from the measured impulse response. The weighing factor α is between 0 and 1. It controls the amount of averaging in the background estimation. This allows emphasizing of recent events, or smoothing out high frequency variations and revealing long term trends in the background estimation. Vector z_k is the signal with subtracted background estimate from the measured impulse

response and represents the result of the background subtraction containing only reflections from moving persons (or other moving objects).

A significant disadvantage of the known background subtraction methods [6], [7], [8], [9] is their poor performance in cases where people are detected according to their azimuthal movement or their breathing or cardiac activity. In these cases, the reflected waves arrive almost in each measured impulse response with the same time delay and are misinterpreted by the detection methods as a static background. People are therefore almost invisible under such circumstances and with such methods. The next section introduces a new adaptive background subtraction method, which removes this drawback.

3. ADAPTIVE BACKGROUND SUBTRACTION

The new proposed background subtraction method is based on the exponential averaging described above. However here, we propose to use instead of a scalar weighing factor α a vector of weighing coefficients α_k . This vector has the size $[N \times 1]$ and is time-variant. Index k refers to the actual time instant. Each vector element α_{ik} (i is from 1 to N) is adaptively controlled as illustrated in Fig. 5.

The vector q_k , which is used to adapt the weighing coefficients α_k , is a result of a background subtraction that is computed in parallel to the “main” signal path. The vector q_k contains information about the time variance of the measured scenario. If there is no moving person, but still there may be a person without movement, it contains only a noise. If there is a time variance, e.g. a person moving in a radial direction to the antennas, there is a strong peak at the appropriate ToF position.

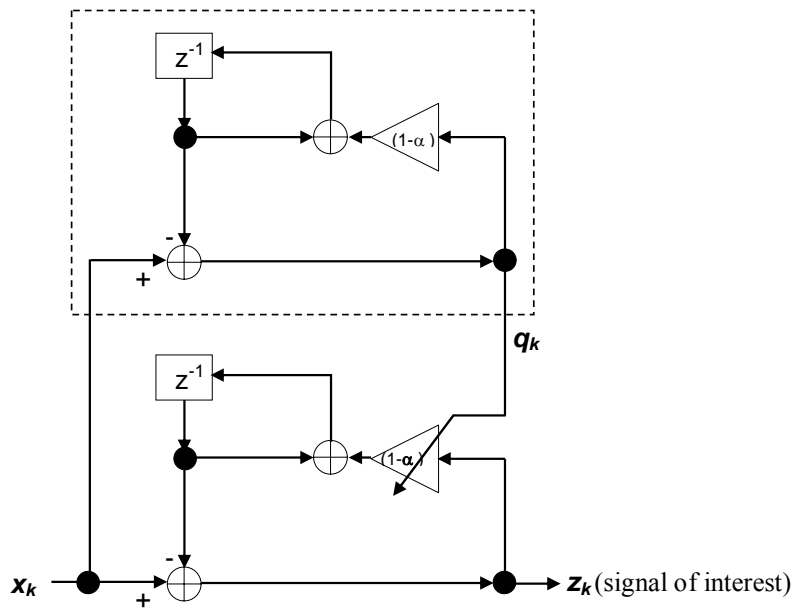


Fig. 5 Adaptive background subtraction based on exponential filtering

This information is used to adapt the vector of weighing coefficients α_k in the following way

$$\begin{aligned}
& \text{if } q_{ik} < \text{Threshold_1} \\
& \quad \text{if } q_{ik}/z_{ik} < \text{Threshold_2} \\
(6) \quad & \quad \quad \alpha_{ik} = 1 \\
& \quad \text{else} \\
& \quad \quad \alpha_{ik} = \alpha \\
& \text{else} \\
& \quad \alpha_{ik} = 1
\end{aligned}$$

Threshold_1 is related to the noise floor of the radar. Variable *Threshold_2* compares vectors \mathbf{q}_k and \mathbf{z}_k and is between 0 and 0.8. If both vectors \mathbf{q}_k and \mathbf{z}_k contain only noise, it means q_{ik} is below *Threshold_1* and the ratio q_{ik}/z_{ik} near to one (above *Threshold_2*), then this hard decision criterion sets all weighing coefficients α_{ik} to the value α . Thus, the background estimate is updated by the new measured impulse response \mathbf{x}_k . As far as vector \mathbf{q}_k contains values above *Threshold_1*, the related weighing coefficients α_{ik} are set to 1 (at the ToF position) and the rest of these coefficients are set to the value α . This assures that the background estimate at the positions where a movement was detected is not updated by waves reflected from a person, which do not belong to the background estimate. Thus, once a moving person is detected, the reflected waves from it are not used for the background estimation. If this person stops or walks further in the azimuth direction, then the ratio q_{ik}/z_{ik} tends to zero (is under the *Threshold_2*). The background estimate at the positions where a person was detected is not updated. Therefore, although the reflections arrive at the same ToF position, they do not count for the background and person detection is successful also in such a case. The performance of conventional and the new adaptive background subtraction method based on exponential filtering will be illustrated by measurement examples later in this article.

4. LOCATION ESTIMATION

The problem description of the simplest case of 2D passive location estimation is illustrated in Fig. 6. The aim is to determine passively only by electromagnetic waves reflected from the person its position using a receive antenna array consisting of two antenna elements.

The localization system estimates firstly round trip times of electromagnetic waves propagating from the transmit antenna Tx towards the person and reflected back from the person towards each of the receive antenna array elements RxN. Estimated round trip times $\tau_{p1}(t) = (s_0(t) + s_1(t))/c$ and $\tau_{p2}(t) = (s_0(t) + s_2(t))/c$ determine two ellipses whose focal points are determined by the locus of the transmit antenna and the loci of the corresponding receive antennas. Thus, the target position results from the intersection of both ellipses described by following equations

$$(7) \quad \left(\frac{x(t) + \frac{D}{2}}{a_1(t)} \right)^2 + \left(\frac{y(t)}{b_1(t)} \right)^2 = 1$$

$$(8) \quad \left(\frac{x(t) - \frac{D}{2}}{a_2(t)} \right)^2 + \left(\frac{y(t)}{b_2(t)} \right)^2 = 1$$

The length of the main axis $2a_i$ is given by the appropriate round trip time τ_{pi}

$$(9) \quad 2a_i(t) = s_0(t) + s_i(t) = c\tau_{pi}(t)$$

and the length of the minor axis $2b_i$ is calculated from

$$(10) \quad \left(\frac{D}{2} \right)^2 + b_i^2(t) = a_i^2(t)$$

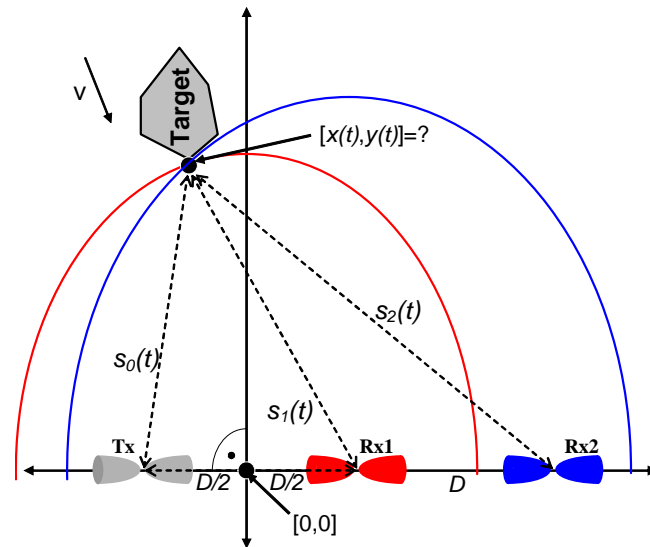


Fig. 6 Positioning - passive approach

The precision of the location estimation depends on the array geometry in connection with the actual locus of the target, the precision of the time delay estimator and also on the design of the radar unit, which has to provide a stable ultra-wideband sounding signal. Furthermore, appropriate antenna models and correction methods are needed if the required precision comes down to the antenna size or even below. Thus, the large bandwidth and good temporal resolution of ultra-wideband localization systems are an essential basis for an accurate positioning calculation, but are not sufficient when the requirements call for extremely accurate devices.

5. M-SEQUENCE RADAR ARCHITECTURE AND DESIGN

The extreme bandwidth, which is necessary to reach a high precision of the location estimation, is not the only requirement posed on the radar system. Apart from this, the basic demands can be summarized as follows:

- a measurement data rate high enough to match the time variance of the scenario due to the movement of people,
- multi-channel arrangement capability in order to allow localization of people,
- a high degree of hardware configuration flexibility to adapt the system performance to the actual requirements of the individual user.

The key to fulfil all these requirements is to use an appropriate stimulation signal. There is a number of excitation signals covering a wide spectral range such as:

- chirp signals,
- stepped sine wave
- short-impulse signals,
- pseudo random binary sequences and others.

The UWB radar, used for the measurement experiments described in the next section, uses binary sequences to stimulate the scenario. From the realisation point of view this stimulus has clear advantages against other UWB signals. For example, apart from its cost, the network analyzer (stepped sine wave signals) can easily meet the UWB bandwidth demand. There is however also some multi-channel arrangement possibility. However, the real-time operation of a network analyser is prohibited by its slow measurement rate. Other systems, e.g. the short-impulse-based systems, offer real-time operation but they are often subjected to a higher susceptibility to jitter and drift.

The stimulation signal of the presented radar is a maximum-length-binary-sequence (MLBS, or M-sequence). MLBS can easily be generated up to tenths of GHz of bandwidth by a digital shift register, which is clocked by a stable single tone RF-oscillator. Besides the advantage of having a reasonable correlation gain, these signals are characterized by small

binary voltage amplitudes that allow extremely fast digital switching in integrated circuit technology to meet the demanding requirements on bandwidth and low jitter.

Fig. 7 presents basic architecture of an UWB radar [11], [12] using M-sequence as a stimulation signal. It is working in the base band covering the spectral band up to half the frequency of the system clock. Controlled by a single tone clock, a digital shift register generates the MLBS signal. Since the MLBS signal is periodical and the measurement scenario can be assumed to be locally stationary, it is possible to acquire the MLBS signal by an under-sampling approach. Here, the binary divider (2^m) determines the under-sampling factor and provides the receiver sampling clock. The measurement data are captured by a Track-and-Hold circuit (T&H), transformed into the digital domain (ADC), optionally synchronously averaged and finally on-line processed or stored for off-line processing. The IR results from an impulse compression, which is performed by the FHT (Fast Hadamard-Transform). The FHT-algorithm is very close to the FFT-algorithm except that it is based on a pure summing of data samples, which promises very fast operation for special hardware implementation. This architecture was used for the development of the UWB through-the-wall radar system for people detection and localization. It covers the band up to 5 GHz and was developed using SiGe monolithic integrated circuits (shift-register, binary divider and T&H). It has been designed by the company MEODAT [13] in cooperation with Ilmenau University of Technology. It consists of one transmitter and two receivers. The extremely linear time axis and the superior jitter and drift behaviour (compared to traditional sequential sampling oscilloscopes) is the result of the synchronous digital controlled sampling. The DSP module of the described experimental systems is based on standard off-the-shelf PCB products. The ADC is a 12-Bit-Video ADC. Fig. 8 shows the radar design, which was constructed in an aluminium briefcase. It contains UWB electronics and three Horn antennas. The antenna side of this suitcase is made of plastic material. The radar system is controlled by a notebook and its graphical user interface is illustrated in Fig. 9. On the right side of the figure, magnitudes of impulse responses measured by 2 receive antennas are depicted. The area on the left side shows the estimated position of a person. The estimation is based on the ToF approach.

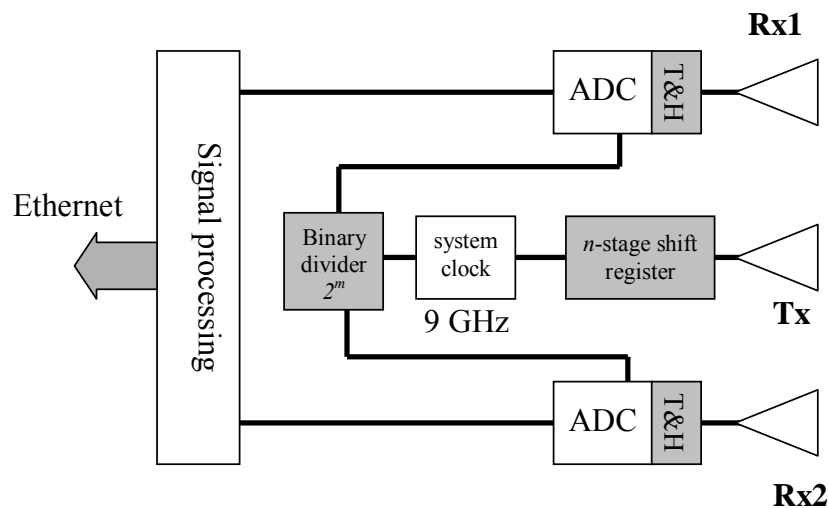


Fig. 7 Architecture of the M-sequence UWB radar



Fig. 8 UWB through-the-wall radar

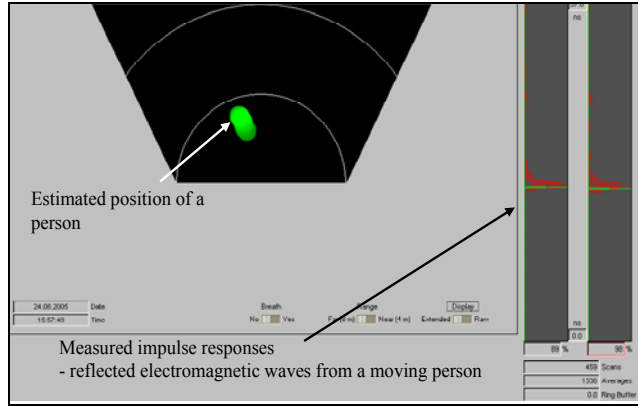


Fig. 9 Graphical user interface

6. MEASUREMENT EXAMPLES

Firstly, we will illustrate the performance of the background subtraction algorithms based on exponential averaging by a measurement example. In this example, a walking person was hidden behind a wall and was walking along the track that is depicted in Fig. 10. The person stopped its movement for a short time in the middle of the cross and at each end of its branches. The walls were about 20 cm thick made of brick. The 2-channel through-the-wall radar described in the previous section was used for the measurement.

Fig. 11 represents unprocessed measured data obtained from one channel of the radar. The vertical axis is related to the time delay and the horizontal axis is related to the time of the measurement. Thus, one vertical line from this 2D figure represents one measured impulse response, which was referred to in the previous equations as a vector \mathbf{x}_k . The unprocessed impulse responses show time variance within the whole measurement only if the person was in a close vicinity to antennas. This is caused by the fact that electromagnetic waves reflected from the walking person are too weak in comparison to antenna cross-talk and the scattering from dominant objects such as walls. The time-variant echo coming from the walking person can hardly be observed directly in measured data.

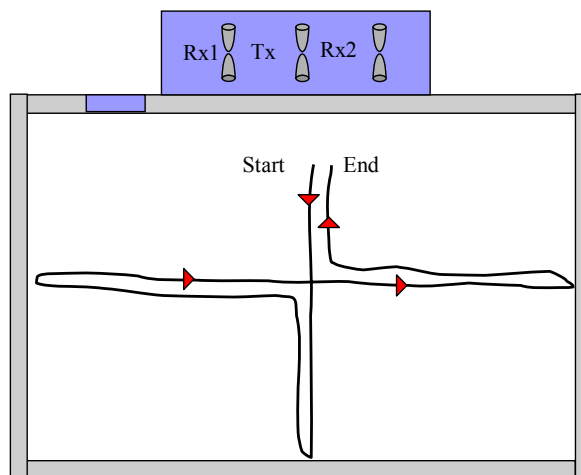


Fig. 10 Measurement scenario

By applying the background subtraction methods we subtract this static background. This brings forward information about the presence of a person in the room and their distance to measurement antennas. Fig. 12 shows the result of the conventional background subtraction computed according to equation (6). In this figure, all impulse responses are normalized so that the maximum value of each impulse response is equal to one. This way we can also observe weak

scattering occurring if the person is far away from antennas. The movement of the person is easy to observe in processed data. The first disadvantage of this method is already visible from Fig. 12. As far as the person does not move, e.g. at the time from 600 to 700 samples, or from 900 to 1100 samples, the reflection from this person vanishes in processed data. This is due to the fact that it counts to the static background that is estimated and then subtracted by this method. Another drawback of this method is the decrease of SNR as far as the motion of the person is slower or, if the person is walking in azimuthal direction with respect to antennas. This is illustrated in Fig. 14. This figure compares SNR of waves reflected from the walking person that are detected by conventional (blue line) and adaptive (red line) background subtraction method. The difference is evident especially as the person is not moving (e.g. time from 35 to 45 seconds). The results of the adaptive background subtraction algorithm computed according to (6) and (7) are presented in Fig. 13. All impulse responses are normalized so that the maximum value of each impulse response is equal to one. The movement of the person was detected also in situations when the conventional method failed to detect waves reflected from the person.

As far as a person is detected by means of its movement or respiratory activity they can be localized by the radar offering

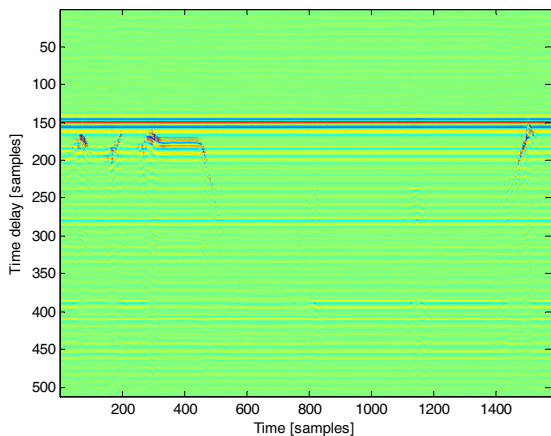


Fig. 11 Measured data

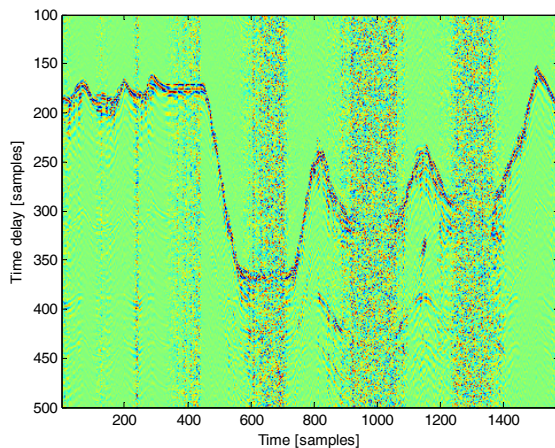


Fig. 12 Data after conventional background subtraction

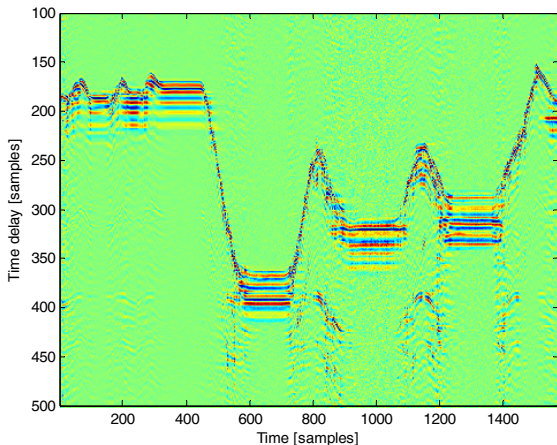


Fig. 13 Data after adaptive background subtraction

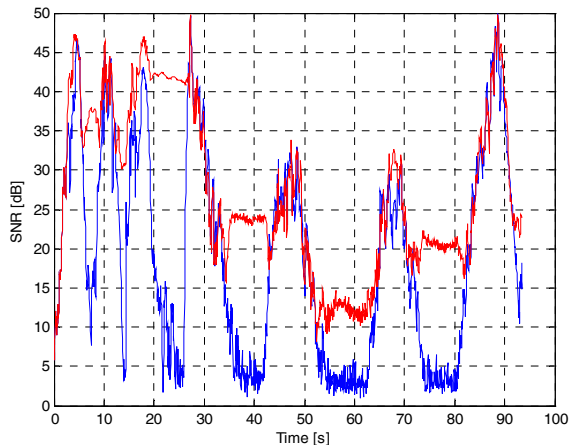


Fig. 14 SNR of the waves reflected from a person and detected by background subtraction algorithms (blue – conventional method, red – adaptive method)

the multi-channel (two Rx antennas) configuration. An example of the through-wall localization is given by the following measurement. The person was walking in a fully equipped office environment. The UWB radar was situated outside the office behind the wall. Just in front of the wall (from the other side) there was a bookcase containing metallic parts.

Firstly, data from each channel were processed by the background subtraction algorithm. Then, ToF between Tx-person-Rx were estimated using a simple threshold detector. The location of the test person was calculated analytically from the estimated ToFs using triangulation principles and imaging technique described in [14], [15]. The office environment and the result of the location estimation is illustrated in Fig. 15.



Fig. 15 Location estimation

7. CONCLUSION

The article presented architecture and design of the UWB through-the-wall radar. Presented algorithms for the detection and subsequent localization were implemented in CVI LabView and operate in real-time. They were tested with the described UWB electronics to detect one person in a static scenario. The achieved precision is in an order of 40cm and can be considered as adequate for the localization of humans. The human body has a certain volume and in the case that arms are fully stretched out, it can have dimensions up to some meters. Thus, it is difficult and unnecessary to define a reference point (e.g. head, heart, belly, etc.) and track it.

In the near future, the performance of the radar will be tested for more challenging scenarios containing more people. It is assumed that presented methods will create the basis for the signal processing of measured data but they must be probably adapted to handle the presence of more people.

REFERENCES

1. R. Benjamin, I. J. Craddock, E. McCutcheon, R. Nilavalan, *Through-Wall Imaging using Real-Aperture Radar*, Conference URSI'02, 2002.
2. Agrawal, B. Fougere, M. Oravakandy, G. Siemens, *Design, Construction, and Testing of a Microwave Radar System for Through-Wall Surveillance*, MSc Thesis, University of Manitoba, Canada, 2004

3. www.millivision.com
4. G. Ohlke, G. Burton, *Exploitation of millimetre waves for through-wall surveillance during military operations in urban terrain*, Report, Canada, 2000
5. *Through-Wall Surveillance For Urban Operation*, Project results, DRDR Ottawa, Canada, 2005
6. M. Piccardi, *Background subtraction techniques: a review*, in Proc. of IEEE SMC 2004 International Conference on Systems, Man and Cybernetics, The Hague, The Netherlands, October 2004.
7. A. McIvor, V. Zang, R. Klette, *The Background Subtraction Problem for Video Surveillance Systems*, International Workshop Robot Vision 2001, Auckland, New Zealand, February 2001.
8. D.J. Daniels, *Ground penetrating radar - 2nd edition*, IEE, London, 2004.
9. A.G. Yarovoy, P. van Genderen, L.P. Ligthart, *Ground Penetrating Impulse Radar for Landmine Detection*, Proc. GPR 2000, SPIE vol. 4084, 8th International Conference on Ground Penetrating Radar, Gold Coast, Australia, 23-26 May, 2000.
10. H. Ebert, J. Sachs, R. Zetik, P. Rauschenbach, *Characterising of Impulse Radiating Antennas*, 48. Internationales Wissenschaftliches Kolloquium, TU Ilmenau, Germany, pp. 20, September 2003.
11. M. Roßberg, J. Sachs, P. Rauschenbach, P. Peyerl, K. Pressel, W. Winkler, D. Knoll, *11 GHz SiGe Circuits for Ultra Wideband Radar*, IEEE Bipolar/BiCMOS Circuits and Technology Meeting, Minneapolis, USA, September 25-26, 2000.
12. J. Sachs, P. Peyerl, M. Roßberg, *A New UWB-Principle for Sensor-Array Application*, IEEE Instrumentation and Measurement Technology Conference, Italy, May, 1999
13. www.meodat.com
14. R. Zetik, J. Sachs, P. Peyerl, *Through-Wall Imaging by Means of UWB Radar*, EUROEM'04, Magdeburg, Germany, 2004.
15. R. Zetik, J. Sachs, R. Thomä, *Imaging of Propagation Environment by UWB Channel Sounding*, XXVIIIth General Assembly of URSI, New Delhi, India, October 23 –29, 2005.